Biochimica et Biophysica Acta 1823 (2012) 2227–2236

Contents lists available at SciVerse ScienceDirect

Biochimica et Biophysica Acta

journal homepage: www.elsevier.com/locate/bbamcr

Involvement of the prostaglandin D2 signal pathway in retinoid-inducible gene 1 (RIG1)-mediated suppression of cell invasion in testis cancer cells

Chang-Chieh Wu [a], Rong-Yaun Shyu [b], Chun-Hua Wang [c], Tzung-Chieh Tsai [d], Lu-Kai Wang [e], Mao-Liang Chen [f], Shun-Yuan Jiang [f], Fu-Ming Tsai [f,*]

[a] Department of Surgery, Tri-Service General Hospital, Taipei 114, Taiwan
[b] Department of Internal Medicine, Buddhist Tzu Chi General Hospital Taipei Branch, New Taipei City 231, Taiwan
[c] Department of Dermatology, Buddhist Tzu Chi General Hospital Taipei Branch, New Taipei City 231, Taiwan
[d] Department of Microbiology, Immunology and Biopharmaceuticals, National Chiayi University, Chiayi, Taiwan
[e] Graduate Institute of Life Sciences, National Defense Medical Center, Taipei 114, Taiwan
[f] Department of Research, Buddhist Tzu Chi General Hospital, Taipei Branch, New Taipei City 231, Taiwan

ARTICLE INFO

Article history:
Received 11 May 2012
Received in revised form 6 August 2012
Accepted 21 August 2012
Available online 30 August 2012

Keywords:
Retinoid-inducible gene 1
Prostaglandin D2 synthase
Testis
HREV107 type II tumor suppressor

ABSTRACT

Retinoid-inducible gene 1 (RIG1), also called tazarotene-induced gene 3, belongs to the HREV107 gene family, which contains five members in humans. RIG1 is expressed in high levels in well-differentiated tissues, but its expression is decreased in cancer tissues and cancer cell lines. We found RIG1 to be highly expressed in testicular cells. When RIG1 was expressed in NT2/D1 testicular cancer cells, neither cell death nor cell viability was affected. However, RIG1 significantly inhibited cell migration and invasion in NT2/D1 cells. We found that prostaglandin D2 synthase (PTGDS) interacted with RIG1 using yeast two-hybrid screens. Further, we found PTGDS to be co-localized with RIG1 in NT2/D1 testis cells. In RIG1-expressing cells, elevated levels of prostaglandin D2 (PGD2), cAMP, and SRY-related high-mobility group box 9 (SOX9) were observed. This indicated that RIG1 can enhance PTGDS activity. Silencing of PTGDS expression significantly decreased RIG1-mediated cAMP and PGD2 production. Furthermore, silencing of PTGDS or SOX9 alleviated RIG1-mediated suppression of migration and invasion. These results suggest that RIG1 will suppress cell migration/invasion through the PGD2 signaling pathway. In conclusion, RIG1 can interact with PTGDS to enhance its function and to further suppress NT2/D1 cell migration and invasion. Our study suggests that RIG1-PGD2 signaling might play an important role in cancer cell suppression in the testis.

1. Introduction

Retinoid-inducible gene 1 (RIG1), also called tazarotene-induced gene 3 (TIG3) or retinoic acid receptor responder 3 (RARRES3) [1–3], is an HREV107 type II tumor suppressor and thereby belongs to the Nlpc/p60 superfamily and the LRAT (Lecithin:retinol acyltransferase)-like family [4,5]. Proteins of this family contain a proline-rich motif located at the N-terminus, followed by a conserved H-box, the NC domain, and a C-terminal transmembrane domain [4,5].

HREV107, RIG1, and HRASLS are involved in the regulation of cellular growth, apoptosis, and differentiation [6–13]. The genes are expressed in normal tissues in a tissue-specific manner, and they are down-regulated in various cancer tissues [14–17]. HREV107 is expressed at high levels in differentiated tissues of post-meiotic testicular germ cells but not human testicular germ cell tumors [15]. Also, terminal differentiation accompanied by the induction of cellular apoptosis and inhibition of cell growth has been observed in keratinocytes after induced RIG1 expression [12,13]. Therefore, the HREV107 protein family appears to play an active role in the regulation of cellular differentiation in both normal and cancer cells.

Cumulative evidence suggests a possible mechanism through which the HREV107 protein family affects cell differentiation and the suppression of cancer progression. Several studies have observed anti-RAS and phospholipid-metabolizing activities among these proteins. Murine H-rev 107 was first isolated from revertants of HRAS-transformed fibroblasts [6]. Subsequently, RIG1, HREV107, and HRASLS were shown to inhibit RAS-mediated signaling of fibroblasts or cancer cell lines [8,10,11,18,19]. Our study further demonstrated a down-regulation caused by RIG1 of activated RAS and total RAS protein, via a posttranslational mechanism [10,11]. Aside from its role in inhibiting RAS activity, the HREV107 protein family could be a phospholipid-metabolizing enzyme. HREV107 catalyzes the efficient release of free fatty acids and lysophospholipid from phosphatidylcholine, indicating that it is a phospholipase A1/A2 [20]. Also, different members of the HREV107 family can react with various

* Corresponding author at: Department of Research, Buddhist Tzu Chi General Hospital Taipei Branch, 289 Jianguo Rd, Sindian District, New Taipei City 231, Taiwan. Tel.: +886 2 6628 9779 5793.
E-mail address: afu2215@gmail.com (F.-M. Tsai).

0167-4889/$ – see front matter © 2012 Elsevier B.V. All rights reserved.
http://dx.doi.org/10.1016/j.bbamcr.2012.08.013

phosphatidylcholines and phosphatidylethanolamines [21]. These results suggest that the tumor suppressors RIG1, HRASLS2, and HREV107 are involved in phospholipid metabolism with different physiological roles.

Prostaglandins (PGs) are lipid-derived autacoids generated by sequential metabolism of arachidonic acid by the cyclooxygenase (COX) and prostaglandin synthase enzymes. Arachidonic acid is a 20-carbon unsaturated fatty acid that esterifies to the sn-2 position of membrane glycerophospholipids. When arachidonic acid is released from the membrane by phospholipase A2, it undergoes oxidation by cyclooxygenase (prostaglandin endoperoxide H synthase, PGHS) to PGG2 followed by reduction to the unstable endoperoxide PGH2 [22]. This intermediate is then switched by different enzymes in the prostanoid biosynthetic pathway. These enzymes are named according to the prostanoid that they produce, such that prostaglandin D2 (PGD2) is synthesized by prostaglandin D synthase (PTGDS), PGF2a by PGFS, PGI2 by PGIS, thromboxane (TXA2) by thromboxane synthase (TXS), and PGE2 by PGES [23]. PGD2 is synthesized in many organs and has been implicated as a signaling molecule in the mediation or the regulation of various biological processes. Previous studies have shown that the *ptgds* gene is male specifically expressed in early stages of mouse gonadogenesis [24]. Furthermore, PGD2 has an effect at the posttranslational level on nuclear translocation of the SRY-related high-mobility group box 9 (SOX9) protein by the cAMP/PKA pathway, subsequently inducing Sertoli cell differentiation [25].

RIG1 stimulates cellular differentiation of keratinocytes, which is mediated by the activation of type I tissue transglutaminase [12,13]. In addition, RIG1 was shown to inhibit RAS signal pathways in cervical and gastric cancer cells [10]. However, the direct interactions of RIG1/Type I tissue transglutaminase or RIG1/RAS were not observed in testicular and cervical cancer cells. Although the HREV107 protein family exhibits activities that can regulate cellular differentiation and suppress cancer cells, the exact mechanism has not been determined. We performed yeast two-hybrid screening and by using the functional NC domain of RIG1 [26] as bait, found that RIG1 can interact with PTGDS. In this study, we showed that RIG1 can suppress cancer cell migration/invasion by interacting with PTGDS and inducing its activity in testicular cell lines. We further dissected the molecular mechanism through which PGD2 suppresses cancer cell migration and invasion. Our results suggest that the invasion and migration abilities of cancer cells are controlled by the expression and interaction of RIG1 and PTGDS.

2. Methods

2.1. Materials

All the chemicals were purchased from Sigma-Aldrich except PGD2, BWA868C, BAY-u3405, and arachidonyl trifluoromethyl ketone (AACOCF3) (Cayman Chemical, Ann Arbor, MI).

2.2. Reverse transcription polymerase chain reaction (RT-PCR)

Total RNA from human tissue was obtained from Clontech (BD Biosciences, Palo Alto, CA). Ten testis RNA samples derived from four normal testes, carcinoma of three testes, and seminoma of three testes were purchased from Origene Technologies (Rockville, MD). cDNA was prepared using M-MLV reverse transcriptase (Invitrogen, Carlsbad, CA) and oligo $(dT)_{12-18}$. Conventional RT-PCR was used to analyze levels of RIG1 and PTGDS expression in human tissues. The PCR reaction was conducted in a 25-μL reaction mixture containing 1 μL of cDNA, 10 mM Tris–HCl (pH 9.0), 50 mM KCl, 0.01% (w = v) gelatin, 0.1% Triton X-100, 2 mM $MgCl_2$, 20 mM dNTP, 100 nM primers for RIG1, PTGDS, or actin, and 1 unit of Pro-Taq DNA polymerase (Protech Technology Enterprise Co., Taipei, Taiwan). The reaction mixtures were subjected to initial 95 °C incubation for 2 min and then amplified for 25 to 35 cycles (94 °C for 30 s, 61 °C for 60 s, and 72 °C for 60 s) in a GeneAmp® PCR System 9700 Thermal Cycler (Applied-Biosystems, Foster City, CA). Five microliters of the amplified product was analyzed by electrophoresis on 2% agarose gel, and images were recorded using the Gel Logic 100 Imaging System (Kodak). Primers used for amplification of RIG1 (5′-AAGTGAGTACCCCGGGGCTGG-3′ and 5′-ACGGGCCGTGGTTGGTACTC-3′), PTGDS (5′-CCGTGCAGCCCAACTTCCAG-3′ and 5′-GCAGCATGGTTCGGGTCTCAC-3′), and actin (5′-TCCCTGGAGAAGAGCTACG-3′ and 5′-GTAGTTTCGTGGATGCCACA-3′) are indicated.

Quantitative real-time PCR was performed in triplicate in 20 μL of a reaction mixture containing 10 μL Fast SYBR Green Master Mix (Applied-Biosystems), 50 ng cDNA, and 100 nM of each primer in a thermal cycler (7900HT Fast Real-Time PCR System, ABI). The PCR cycling comprised an initial incubation at 95 °C for 3 min, 40 cycles of denaturation at 95 °C for 15 s, and annealing and extension at 60 °C for 1 min. Expression data were normalized on the mean of actin gene expression data.

2.3. Expression vectors

The vectors pRIG1-myc, pRIG1ΔC-myc, pDsRed-RIG1, and pDsRed-RIG1ΔC have been described previously [10,26]. To generate pPTGDS-Flag, the PTGDS cDNA fragment was amplified from pPTGDS/PACT2 using 5′ (5′-TGGCTAGCATGGCTACTCATCACACGCTGTG-3′) and 3′ (5′-CGGAATTCGTTGTTCCGTCATGCACTTATCG-3′) primers, and then subcloned in-frame into *Nhe*I-*Eco*RI of PCR3.1-Flag. To generate pEGFP-PTGDS, the PTGDS cDNA fragment was amplified from the pPTGDS-Flag using 5′ (5′-TCGAATTCTATGGCTACTCATCACACGCTGTG-3′) and 3′ (5′-GTGGATCCTTGTTCCGTCATGCACTTATCG-3′) primers, and then subcloned in-frame into *Eco*RI-*Bam*HI sites of the pEGFP-C1 vector (Clontech Laboratories Inc., Palo Alto, CA). The cDNA sequences of fusion proteins were confirmed by DNA sequencing.

2.4. Cell culture and transfection

NT2/D1 testicular cancer cells were maintained in Dulbecco's Modified Essential Medium (DMEM) supplemented with 25 mM HEPES, 26 mM $NaHCO_3$, 2 mM L-glutamine, penicillin (100 units/mL), streptomycin (100 μg/mL), and 10% fetal bovine serum (FBS) at 37 °C in 5% CO_2. Cells plated in culture dishes were transfected with the expression vectors using liposome mediated-transfection. Briefly, plasmids and lipofectamine 2000 (Gibco BRL, Gaithersburg, MD) were diluted in Opti-MEM medium and then mixed with plasmids at room temperature for 15 min. The DNA–lipofectamine complexes were then added to cells for 5 h at 37 °C. Cells were refreshed with complete medium for 24 h at 37 °C for further analysis.

2.5. Analysis of cell death and viability

Cells were plated in triplicate in 24-well plates at a density of 2×10^4 cells per well in DMEM medium containing 10% FBS and were incubated overnight. The cells were transfected with 500 ng of RIG1, RIG1ΔC expression vectors, or empty control vector and then refreshed with complete medium immediately and 24 h after transfection. Cells were analyzed for viability using the WST-1 reagent (100 μL Roche Diagnostics, Mannheim, Germany). Cell viability relative to that of control transfected cells was defined as [(A450–A660) of RIG1-transfected cells/(A450–A660) of control transfected cells] × 100%. Measurement of the release of lactate dehydrogenase (LDH) using the Cytotoxicity Detection Kit (Roche) was used to evaluate cell death as described previously [26]. Percentage LDH release was defined as [(A490–A650) of RIG1-cells/(A490–A650) of control transfected cells] × 100%.

2.6. Cell migration and invasion assay

For cell migration assay, 2×10^4 NT2/D1 cells were added to the upper polycarbonate membrane insert (8 μm pore size; Falcon, Becton Dickinson) of the cell migration assay kit in a 24-well plate. In the lower well, 700 μL DMEM with 20% FBS was used as chemoattractant. After 24 h of incubation, cells were methanol fixed for 10 min at room temperature and then stained for 30 min at room temperature with a 50 μg/mL solution of propidium iodide (Sigma-Aldrich). Polycarbonate-membrane inserts coated with 30 μg Matrigel (BD) were used for cell invasion assays. NT2/D1 cells were suspended in DMEM medium containing 10% NuSerum (Invitrogen). 2×10^4 cells were placed in the upper chambers, and 700 μL of medium was placed in the lower chambers. After incubation for 72 h at 37 °C, cells were fixed and stained for propidium iodide. The number of cells on each membrane was counted under a microscope at a magnification of 40×. Experiments were performed at least twice, and each sample was assayed in triplicate.

2.7. Immunoprecipitation, nuclear and cytoplasmic fractionation, and Western blotting

Cells were lysed in IP lysis buffer (20 mM Tris–HCl at pH 7.5, 100 mM NaCl, 1% Nonidet P40, 100 μM Na_3VO_4, 50 mM NaF, 30 mM sodium pyrophosphate) containing 1× complete protease inhibitor cocktail (EDTA-free) (Roche). Cell lysates containing 500 μg of protein were incubated first with 3.2 μg of anti-myc (Invitrogen) or 1 μg of anti-Flag-M2 (Sigma-Aldrich) monoclonal antibody for 2 h at 4 °C, and then incubated with 20 μL of protein G plus/protein A agarose (Calbiochem, Cambridge, MA) at 4 °C for 2 h. Immunoprecipitated complexes were washed three times with IP lysis buffer and then analyzed by Western blotting using an anti-myc or anti-Flag antibody. Alternatively, cell lysates containing 5 mg of protein were incubated first with 4 μg of normal rabbit IgG (Santa Cruz Biotechnology, Santa Cruz, CA), 4 μg of anti-RIG1 (Santa Cruz Biotechnology), or 4 μg of anti-PTGDS (Santa Cruz Biotechnology) antibody for 12 h at 4 °C and then incubated with 20 μL of protein G plus/protein A agarose (Calbiochem) at 4 °C for 2 h. Immunoprecipitated complexes were washed three times with IP lysis buffer and then analyzed by Western blotting using anti-RIG1 (Santa Cruz Biotechnology) or anti-PTGDS (Abcam, Cambridge, UK) antibody. To determine the nuclear or cytosolic distribution of SOX9, cell fractionation was performed using the Qproteome cell compartment kit (Qiagen, Valencia, CA) according to the manufacturer's instructions with the addition of protease and phosphatase inhibitors to all buffers. For Western blotting, proteins (20–50 μg) were separated on 12% polyacrylamide gels and transferred to polyvinylidene difluoride membranes. After blocking, membranes were incubated with anti-myc, anti-Flag, anti-PTGDS (Abcam), anti-phospho-SOX9 (Abcam), anti-SOX9 (Abcam), anti-lamin B1 (Invitrogen), anti-glyceraldehyde 3-phosphate dehydrogenase (GAPDH) (Cell Signaling Technology, Beverly, MA), or anti-actin (Sigma-Aldrich) antibody for 12 h at 4 °C, and then incubated with horseradish peroxidase-conjugated goat anti-mouse antibody at room temperature for 1 h. An ECL kit (Amersham, Bucks, UK) was used to detect the substrate reaction.

2.8. Confocal and immunofluorescent analysis

NT2/D1cells (1×10^5) were plated on poly-L-lysine-coated coverslips in 35-mm dishes in growth medium. Cells were then transfected with 500 ng of DsRed-RIG1 or pDsRed-RIG1ΔC with 500 ng pEGFP-PTGDS expression vector for 18 h. The cells were washed and fixed with 4% paraformaldehyde and then analyzed with a Leica TCS SP5 scanner (Leica, Bensheim, Germany).

2.9. Measurement of PGD2 and cAMP levels

Cells were cultured onto 6-well plates overnight and then transfected with 500 ng pPTGDS-Flag along with 500 ng of pRIG1-myc, pRIG1ΔC-myc, or control vector in complete medium for 24 h or treated with PGD2 (500 ng/mL) for 30 min, 1 mM Br-cAMP for 18 h. After washing twice with PBS, cells were lysed with 0.1 N HCl for 20 min, scraped, and collected by centrifugation. Levels of PGD2 or cAMP in the supernatants were determined using a prostaglandin D2 express or cyclic AMP EIA kit (Cayman Chemical) according to the manufacturer's instructions.

2.10. Viruses and transduction

LacZ, PTGDS, and SOX9-shRNA-containing lentiviral vectors were obtained from the National RNAi Core Facility (Academia Sinica, Taiwan) and prepared in accordance with standard protocols. Cells were infected with lentivirus (multiplicity of infection 5) in medium containing polybrene (8 μg/mL). Three PTGDS shRNAs targeted to nucleotides 540 to 560 (5′-CAGGGCTGAGTTAAAGGAGAA-3′), 590 to 611 (5′-CACAGAGGATACCATTGTCTT-3′), and 625 to 645 (5′-GATA AGTGCATGACGGAACAA-3′) were synthesized based on Genbank accession NM_000954. Three SOX9 shRNAs targeted to nucleotides 1234 to 1253 (5′-ACCTTCGATGTCAACGAGTTT-3′), 1761 to 1781 (5′-GATAAGTGCATGACGGAACAA-3′), and 3680 to 3700 (5′-GCATCC TTCAATTTCTGTATA-3′) were synthesized based on Genbank accession NM_000346.

3. Results

3.1. RIG1 and PTGDS were highly expressed in normal testis tissue

The RIG1 and PTGDS expression profiles in normal and cancer tissue were analyzed by in silico data mining, using mRNA expression data from the GeneNote database (http://bioinfo2.weizmann.ac.il/cgi-bin/genenote/home_page.pl). This analysis showed that both RIG1 and PTGDS mRNA were highly expressed in normal lymph node, spinal cord, lung, liver, testis, and placenta tissues. Lower expression of RIG1 and PTGDS mRNA was observed in cancer tissues derived from the above tissue types (Fig. 1A). The expression levels of RIG1 and PTGDS were confirmed in 13 normal tissues using conventional RT-PCR. High expression levels of both RIG1 and PTGDS cDNA, at 150 bp and 201 bp in length, respectively, were amplified from cDNA derived from normal tissues of brain and testis after 35 cycles of amplification (Fig. 1B). Higher expression of RIG1 and PTGDS mRNA in brain and testis tissues was confirmed using quantitative real-time PCR analysis (Fig. 1C). Although the gene expressions of RIG1 and PTGDS in silico data are somewhat different from our results in different tissues, high expressions of both RIG1 and PTGDS in testis tissue are consistent with that in in silico data. Human testis cell samples from normal cells, testicular embryonal carcinoma, and testicular seminoma were used to clarify the expression of RIG1 and PTGDS in order to confirm that RIG1 and PTGDS are expressed in these testis samples (Fig. 1D). Quantitative real-time PCR analysis showed that the gene expression of RIG1 and PTGDS in the normal cells was higher than that in the carcinoma (*RIG1* $p<0.001$, *PTGDS* $p=0.002$) or seminoma (*RIG1* $p<0.001$, *PTGDS* $p=0.003$) testis cancer cells (Fig. 1E). The result seems to implicate RIG1 and PTGDS in the regulation of cell function in testis cells and possibly in the inhibiting of testicular carcinogenesis.

3.2. RIG1 suppresses migration and invasion of NT2/D1 testis cells

The members of the HREV107 protein family exhibit growth-suppressive activities in various cancer lines [6,26,27]. Therefore,

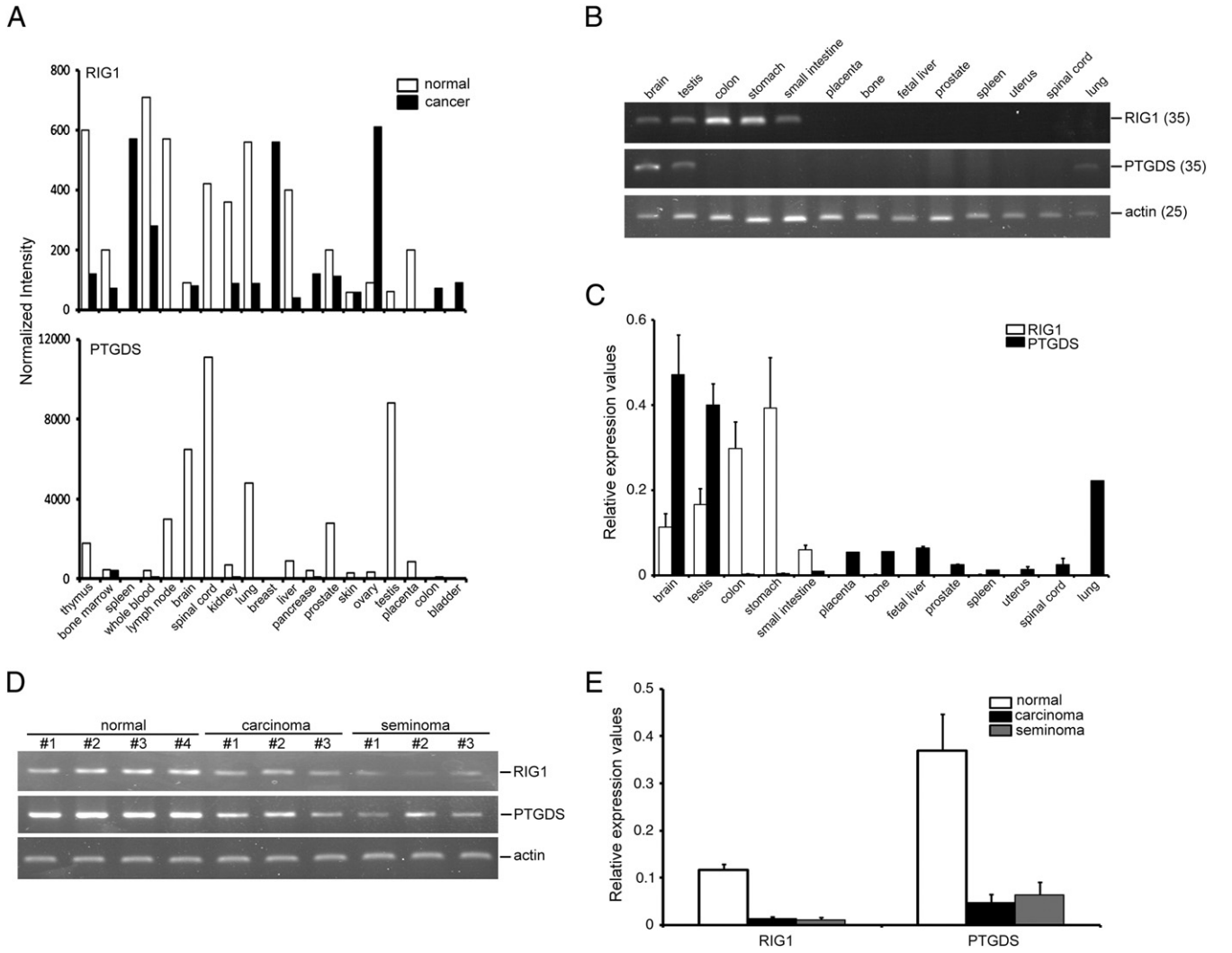

Fig. 1. RIG1 and PTGDS were highly expressed in testis normal tissues. The analysis of mRNA expression of RIG1 and PTGDS in different normal and cancerous tissues was modified from the GeneNote database (A). cDNA derived from total RNA of normal human tissues was prepared. Expression of RIG1 and PTGDS was analyzed by conventional RT-PCR (B) or quantitative real-time PCR (C). Expression of actin served as the control. Cycles of PCR are indicated in parentheses. Total testis RNA derived from four normal, three carcinoma, or three seminoma were purchased from Origene technologies and cDNA were prepared. The expression of RIG1 and PTGDS in normal and cancer tissue of testis was assessed by conventional RT-PCR (D) or quantitative real-time PCR (E). Expression values are normalized on the mean of actin gene expression.

we investigated the involvement of RIG1 proteins in the growth and death of NT2/D1 testis cancer cells. Overexpression of RIG1 or a transmembrane-spanning C-terminus truncated with RIG1 (RIG1ΔC) in NT2/D1 cells did not appear to influence cell death or viability (Fig. 2, A and B). However, we observed a dramatic decrease in migrated and invaded cells by 44% and 59%, respectively, in RIG1-expressing NT2/D1 cells (Fig. 2, C and D). Truncation of RIG1 at the C-terminus (RIG1ΔC) resulted in complete loss of the activity that suppresses cell migration and invasion in NT2/D1 cells.

3.3. RIG1 associates and co-localizes with PTGDS

In a previous study, we carried out a yeast two-hybrid analysis to identify the interaction of the NC domain of RIG1 and PTGDS. Their interaction was further confirmed in NT2/D1 cells. We performed co-immunoprecipitation, using anti-myc antibody against the myc epitope of RIG1 fusion proteins and using lysates of PTGDS-Flag transfected NT2/D1 cells. The PTGDS protein was demonstrated on immunoblots from RIG1 but not from RIG1ΔC co-transfected immunoprecipitates, indicating the presence of PTGDS in the RIG1 pull-down protein complexes prepared in vitro (Fig. 3A). Similarly, RIG1 but not RIG1ΔC was present in the PTGDS immunoprecipitates (Fig. 3B). It is surprising that RIG1ΔC containing NC domain did not interact with PTGDS, which suggests that RIG1 may interact with PTGDS in a constricted space. Truncation of the C-terminus of RIG1 led to homogenous distribution and complete loss of binding activity. To further validate the endogenous interaction of RIG1 and PTGDS, we performed co-immunoprecipitation, using anti-RIG1 or anti-PTGDS antibodies in NT2/D1 cell lysates. Our result revealed that endogenous RIG1 can interact with PTGDS (Supplemental Fig. 1).

To further verify the co-localization of RIG1 and PTGDS in vivo, we co-transfected NT2/D1 cells with pEGFP-PTGDS and various pDsRed-RIG1 expression vectors. Eighteen hours after transfection, EGFP-PTGDS was localized in the perinuclear region. DsRed-RIG1 fusion protein was primarily distributed in the discrete compartment of the perinuclear region, where DsRed-RIG1would co-localize (yellow) with EGFP-tagged PTGDS protein (Fig. 3C). DsRed-RIGΔC was distributed homogenously within the cell and showed no co-localization with EGFP-PTGDS, which localized predominantly in the perinuclear region.

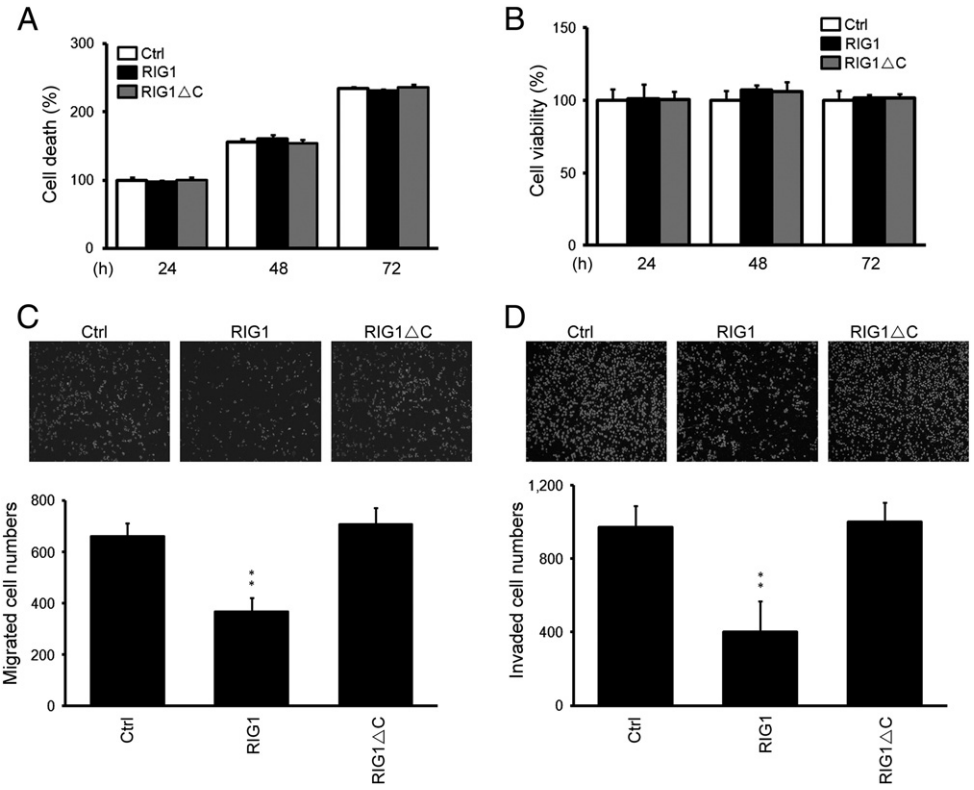

Fig. 2. RIG1 suppresses cell migration and invasion. NT2/D1 cells plated in triplicate in 24-well plates were transfected with 500 ng of myc-tagged RIG1 expression vectors for 3 days. Cell death and cell viability were detected by LDH release (A) and WST-1 assay (B), respectively. Representative results of three independent experiments are shown and expressed as average and standard error of the means after normalization with the control group at 24 h. Serum-starved cells in triplicate were added in upper polycarbonate membrane inserts in 24-well plates. Lower wells contained 700 μL of DMEM with 20% FBS, which was used as chemoattractant. Migratory cells were stained after 24 h of incubation (C). Invasive ability was measured with the Matrigel invasion assay after 72 h of incubation. Representative results of three independent experiments are shown (D). Student's t-test: ** $P<0.01$.

3.4. RIG1 enhances PTGDS activity

To examine the effect of RIG1 on PTGDS activity, NT2/D1 cells were co-transfected with the PTGDS expression vector and the RIG1, RIG1ΔC, or control vector. Twenty-four hours after transfection, expression of PGD2 was induced specifically by activation of PTGDS as determined by EIA detection. Expression of PTGDS increased PGD2 levels in NT2/D1 cells by 39%. In NT2/D1 cells co-transfected with PTGDS and RIG1, PGD2 levels increased by 193% (Fig. 4A). Expressing only RIG1 in NT2/D1 cells enhanced PGD2 expression by 117%.

Expression levels of cAMP and SOX9, which were stimulated by the PGD2 produced by PTGDS, were also examined in RIG1-expressing cells. PGD2 elevated intracellular cAMP levels in NT2/D1 cells (Fig. 4B). cAMP production was increased by 43% in PTGDS-expressing cells and reached a 69% when RIG1 was co-expressed. Expressing RIG1 only in NT2/D1 cells did enhance the cAMP levels by 52%. Cells treated with Br-cAMP, a stable cAMP analogue, showed expression change of SOX9 by 3.8-fold when compared to control cells (Fig. 4C). Also, RIG1 enhanced the expression of SOX9 in NT2/D1 cells by 4.7-fold. The activation of SOX9 was involved in both the nuclear translocation and PGD2-induced, cAMP-activated, PKA-mediated phosphorylation of SOX9 [25]. In order to determine the activated status of SOX9 expression up-regulated in RIG1-expressing cells, we next analyzed whether RIG1 affects SOX9 subcellular distribution, using cell fractionation results in NT2/D1 cells. Also, both SOX9 and phosphorylated SOX9 were up-regulated and were detected exclusively in the nucleus fraction of cells that were treated with Br-cAMP or expressed RIG1 (Fig. 4D). RIG1ΔC eliminated the interaction of PTGDS and the ability to induce PGD2, cAMP production and SOX9 activation in NT2/D1 cells (Fig. 4, A–C). These results revealed that PGD2 expression was up-regulated in RIG1-expressed cells. Furthermore, the expression of PGD2 induced the production of cAMP and the activation of SOX9.

Because RIG1 can enhance PTGDS activity, the effect of PTGDS on RIG1-mediated RAS suppression in cervical cells was also examined. The EGF-stimulated Ras-GTP level was suppressed in cells transfected with the RIG1 expression vector. RIG1 was observed to enhance PTGDS activity in NT2/D1 cells. In contrast, PTGDS was observed to inhibit RIG1-mediated RAS suppression in a dose-dependent manner (Supplemental Fig. 2) in HtTA cells. The result suggests that PTGDS might interact with RIG1 and that this subsequently blocked the complex formation of RAS and RIG1.

3.5. Silencing of PTGDS and SOX9 expression decreases RIG1-mediated suppression of cell migration and invasion

Previous studies have confirmed that the HREV107 protein family acts as a phospholipase A, which can release free fatty acids and lysophospholipid from phosphatidylcholine [20,21]. Also, phospholipase A activity is required for PTGDS-mediated PGD2 production in mast cells [28,29]. We used a known PLA1/2 inhibitor, AACOCF3, to determine the role of phospholipase activity in the effect of RIG1 on the PGD2 pathway. Inhibition of PLA1/2 by AACOCF3 had no effect on RIG1-induced PTGDS activity, cell migration, or invasion (Supplemental Fig. 3). This result suggests that phospholipase activity is not required for the induction of RIG1-mediated PTGDS activity.

To determine whether the PGD2 pathway contributes to RIG1-mediated suppression of cancer cell migration/invasion, we examined the effects of PTGDS- and SOX9-silencing on the production of PGD2

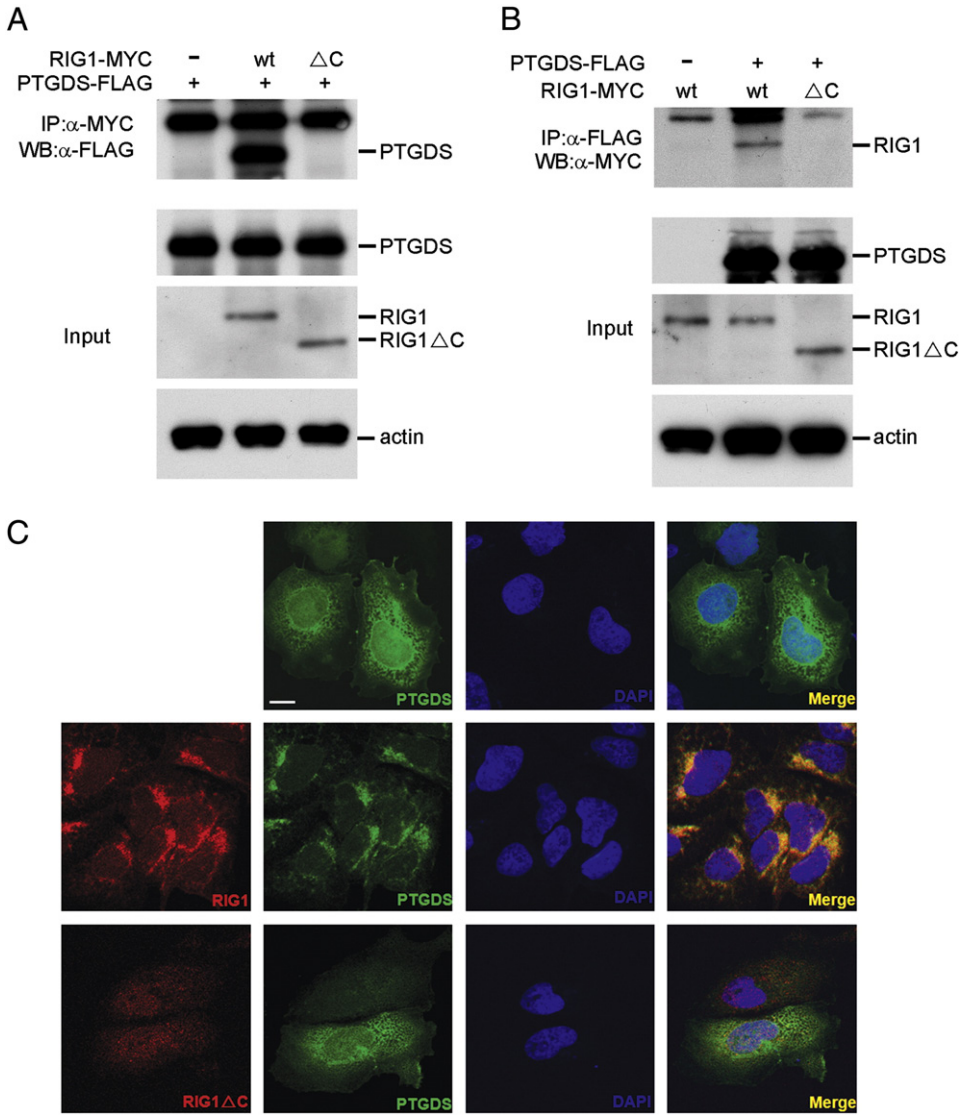

Fig. 3. RIG1 associates and co-localizes with PTGDS. NT2/D1 cells plated in a 10-cm dish were transfected with 3 μg PTGDS-Flag along with the RIG1-myc or RIG1ΔC-myc expression vector or with the control vector for 24 h. The cell lysates were prepared, and the interaction between RIG1 and PTGDS was analyzed by immunoprecipitation followed by Western blot analysis. Immunoprecipitates were resolved by SDS-PAGE and immunoblotted using the anti-Flag antibody (A) or anti-myc antibody (B). The levels of total PTGDS, RIG1, and actin in the cytosolic extracts were detected by Western blotting. NT2/D1 cells were cotransfected with EGFP-PTGDS and either DsRED-RIG1 or DsRED-RIG1ΔC expression vectors for 18 h. Cells were fixed, stained with DAPI, and analyzed with a laser scanning confocal microscope (C). Scale bar: 10 μm.

and cAMP, cell migration, and invasion in RIG1-expressing cells. NT2/D1 cells were transducted with three different shRNAs to inhibit PTGDS or SOX9 expression. As shown in Fig. 5, A and B, expression of PTGDS in NT2/D1 cells was suppressed when transducted with the PTGDS-1 or PTGDS-3 shRNAs. SOX9 expression was suppressed in each of three SOX9 shRNA-transfected NT2/D1 cells. The expression of neither PTGDS nor SOX9 was affected when cells were transducted with LacZ shRNA. Our results showed that PGD2 and cAMP expressions were markedly decreased (suppression ranging from 44.7 to 58% and from 44.1 to 49.3%, respectively) in PTGDS shRNA-silencing cells (Fig. 5C). Furthermore, expression level of RIG1-stimulated SOX9 was 51.5 to 74.1% lower than that of LacZ-silencing cells (Fig. 5D). Although SOX9 shRNAs did not affect RIG1-mediated PGD2 or cAMP production, both PTGDS- and SOX9-silencing shRNAs alleviated the suppression of RIG1-mediated cell migration and invasion (Fig. 5, E and F). Thus, our results suggest that RIG1 could suppress cell migration and invasion in testis cancer cells by affecting PGD2 signaling pathways.

3.6. RIG1-induced suppression of cell migration and invasion is accomplished by the PGD2 signaling pathway via stimulation of DP1 receptor

The biological effects of PGD2 are transduced by D prostanoid receptor (DP) 1 and DP2. To determine the mechanisms by which RIG1 affects PGD2 inhibition of cell migration and invasion, we examined intracellular cAMP levels after treating cells with DP antagonist. Increased PGD2 expression was observed in RIG1-expressing cells. This would not be affected by cells treated with DP1 antagonist BWA868C or DP2 antagonist BAY-u3405. However, RIG1 can significantly elevate intracellular cAMP levels and SOX9 expression that would be blocked by BWA868C but not by BAY-u3405 (Fig. 6, A and B). These results suggest that DP1 receptor participates in the inhibition processes of SOX9 expression. Cell migration and invasion were suppressed, respectively, in PGD2-treated (89.2% and 89.7%) and RIG1-expressing (63.3% and 52.8%) NT2/D1 cells (Fig. 6, C and D). Our results also showed that only BWA868C prevented the suppression of RIG1-mediated cell migration and invasion (Fig. 6, C and

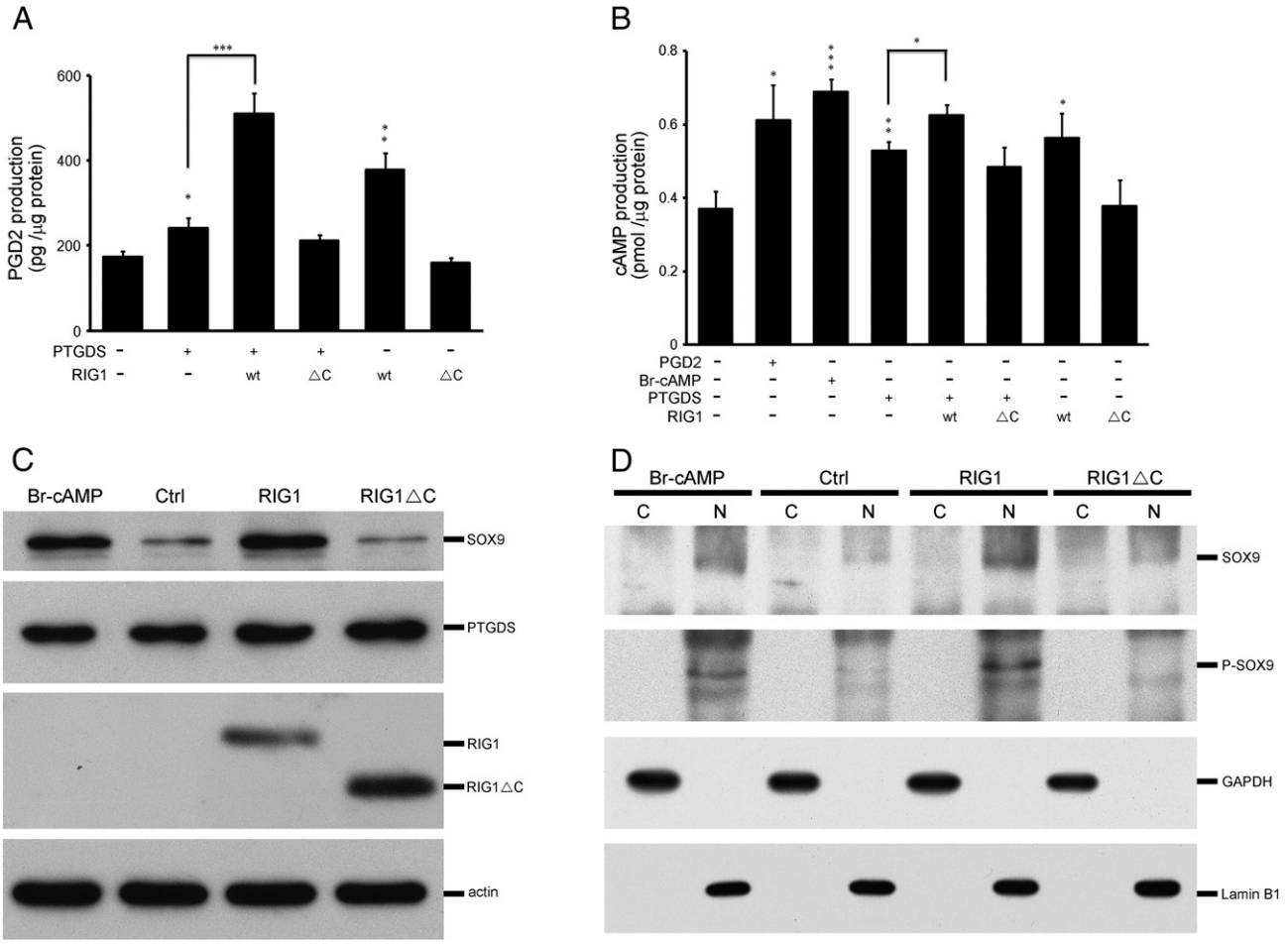

Fig. 4. RIG1 increases PGD2 and cAMP levels and enhances PGD2-mediated SOX9 subcellular localization. NT2/D1 cells plated in triplicate in 6-well plates were transfected with 1 μg PTGDS-Flag along with RIG1-myc or RIG1ΔC-myc expression vector for 24 h. Alternatively, the cells were treated with 1 mM Br-cAMP for 18 h or 500 ng/mL PGD2 for 1 h. Cell lysates were prepared, and levels of PGD2 (A) or cAMP (B) were measured using an enzyme immunoassay. Representative results from triplicate samples were expressed as mean ± SD. *, $P<0.05$; **, $P<0.01$; ***, $P<0.001$. Cells were transfected with RIG1 or RIG1ΔC expression vector for 24 h or treated with 1 mM Br-cAMP for 18 h. Expression of SOX9 was determined by Western blot analysis using anti-SOX9 antibody (C). Cells were transfected with RIG1 or RIG1ΔC expression vector for 24 h or treated with 1 mM Br-cAMP for 18 h. Nuclear and cytosolic fractions were prepared, and subcellular distribution of nuclear and cytosolic SOX9 and phosphorylated SOX9 was determined by Western blot analysis (D).

D). A similar alleviation of PGD2-suppressed migration and invasion was also observed in cells treated with BWA868C (data not shown).

4. Discussion

Our results indicate that ectopic RIG1 in testis cancer cells may serve as a PTGDS activator that regulates the PGD2 pathway and cancer migration and invasion. We found that expression of RIG1 in NT2/D1 cells suppresses cell migration and invasion and enhances PTGDS-induced PGD2 production. We suspect that expression of RIG1 in NT2/D1 cells might directly or indirectly affect the DP1 receptor and downstream signaling pathway to further elevate cAMP levels and SOX9 activation. We also observed reversion of RIG1-mediated migration and invasion suppression in PTGDS- and SOX9-silenced NT2/D1 cells after transduction with shPTGDS and shSOX9. A similar result was observed in cells treated with DP1 antagonist BWA868C. Emerging evidence has suggested that RIG1 specifically regulates cancer migration/invasion, through the PGD2 signaling pathway (Fig. 7).

RIG1 belongs to the HREV107 type II tumor suppressor family, which regulates cellular apoptosis, differentiation, and growth suppression. Previous studies have focused on the effects of the HREV107 protein family in suppressing RAS-mediated transformation in cancer cells [6,8,10,11,19,27]. Although the anti-RAS effect induced by HREV107 protein family has been verified, the direct interaction of RAS and RIG1 in cancer cells has not been observed [11]. The literature scarcely mentions the relationship between RAS and the differentiation of testis tissue even though PTGDS can suppress RIG1-mediated RAS suppression. In contrast, the PGD2 pathway is well-known in testis differentiation in the mouse model [25,30,31]. PGD2-induced regulation of cell differentiation and suppression of migration and invasion in cancer cells have also been reported [32–34]. PGD2 is known to stimulate cAMP production to inhibit TGF-β1-induced epithelial-to-mesenchymal transition by up-regulating E-cadherin in Madin–Darby canine kidney cells [32]. Whether the expression of E-cadherin is regulated by SOX9 needs further investigation. PGD2 and cAMP participate in multiple signaling pathways, which may explain why the reversion of RIG1-mediated suppression of migration and invasion in RIG1-expressing cells was slightly higher using PTGDS shRNAs than with cells transfected with SOX9 shRNA (migration p-value = 0.004, invasion p-value = 0.032) (Fig. 5, E and F). Previous studies have indicated that combined treatment with PGD2 and retinoic acid substantially decreases tumor growth in human ex vivo and mouse in vivo models of melanoma [35]. Interestingly, RIG1 is retinoid acid-inducible, which suggests that RIG1 might be inclusive in retinoid acid-mediated testicular tumor suppression [36,37].

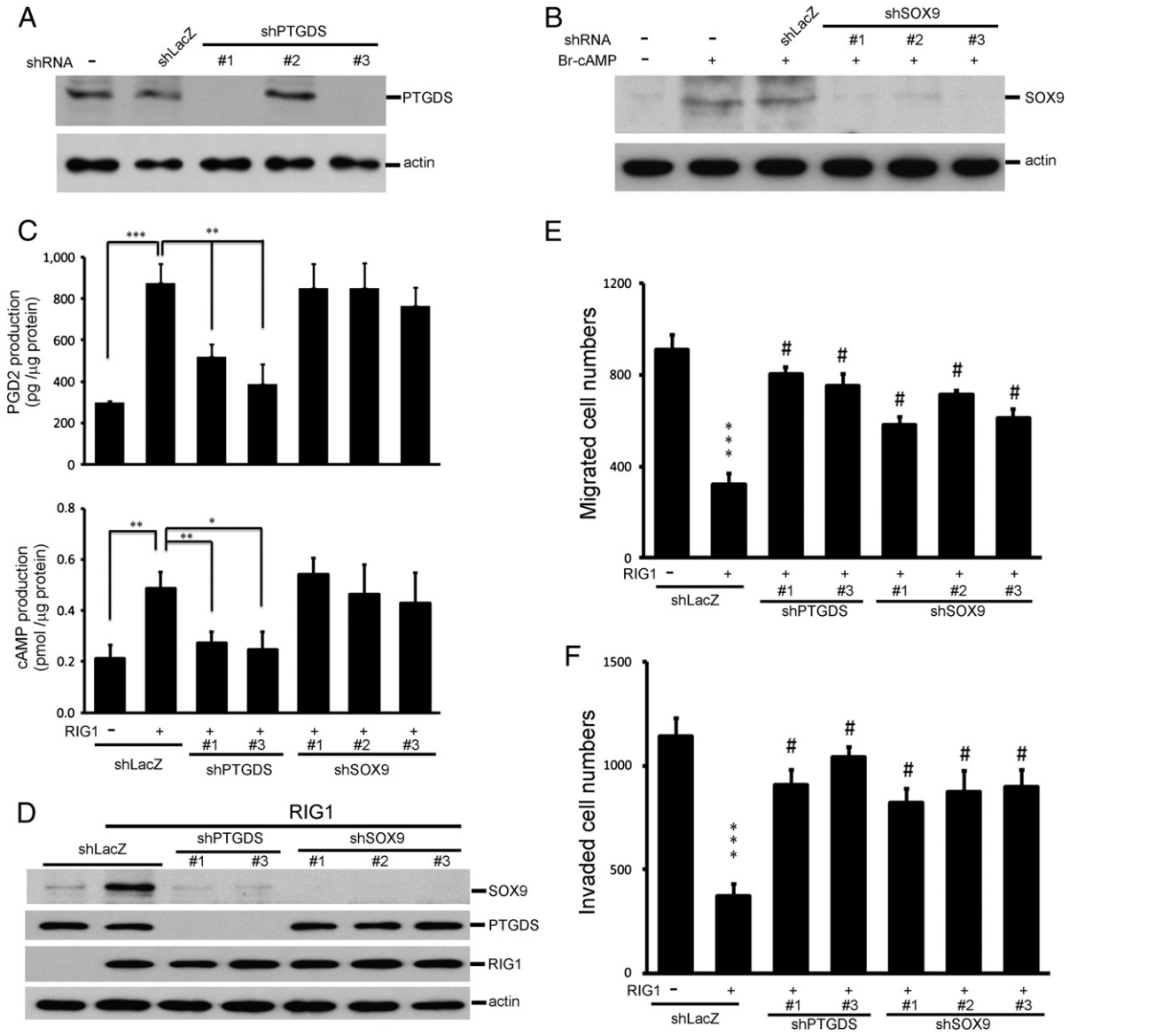

Fig. 5. PTGDS and SOX9 shRNAs alleviate the RIG1-mediated suppression of migration and invasion. NT2/D1 cells were transducted with the indicated shRNAs for 72 h, cell lysates were prepared, and the expression of PTGDS (A) or SOX9 (B) was determined using anti-PTGDS or anti-SOX9 antibodies. Cells were transducted with indicated shRNA for 72 h and then transfected with RIG1 expression vector for 24 h. The levels of PGD2 and cAMP were determined using an enzyme immunoassay (C), and expression of SOX9 was determined by Western blot analysis using anti-SOX9 antibody (D). Representative results from triplicate samples were expressed as means ± SD. Migration (E) and invasiveness (F) were determined in cells transduced with indicated shRNA. Representative results of three independent experiments are shown. Student's t-test: *, $P<0.05$; **, $P<0.01$; ***, $P<0.001$ versus control; #, $P<0.01$ versus RIG1-expressing cell that transducted with shLacZ.

There is little discussion in the literature concerning the relationship between cell migration/invasion and the PGD2-SOX9 signal pathway in testis cells. Contrary to our study, SOX9 might be an oncoprotein and its expression has been linked to urothelial carcinoma cell-lines invasion [38]. Other research results have mentioned the role of SOX9 in cell differentiation. SOX9 has been shown to directly bind CREB as a novel synergism with the protein kinase A pathway in BMP-2-induced osteochondrogenic differentiation [39]. Also, PGD2 synergizes cAMP and induces SOX9 activation and subsequent Sertoli cell differentiation [25,40]. The results show that the combination of SOX9 and a different signal pathway will alter cell function.

According to our results, the interaction of the HREV107 protein family with PTGDS might play an important role in testis cell development or differentiation when RIG1 and PTGDS co-express and co-interact in the testis cell (Fig. 7). Our hypothesis is supported by the following: (1) high mouse H-rev107 (RIG1 homology protein) expression levels in differentiated testicular tissues in mice suggests that H-rev107 expression is correlated with testicular development [15]; (2) expression of PTGDS has been detected in the cellular lineage that gives rise to Sertoli cells [41], and the Sertoli cells appear to express PGD2 synthase only during stages VI–VIII of the spermatogenic cycle, immediately after spermiation [42]; (3) PGD2 can induce SOX9 nuclear translocation and subsequent Sertoli cell differentiation [25]; and (4) we identified the RIG1-binding protein using the NC domain of RIG1, and the domain is highly homologous with another HREV107 protein family. By comparing amino acid sequences of RIG1 with mouse H-rev107, we found that 39% of their amino acids are identical. This suggests that mouse H-rev107 might interact with PTGDS due to its similarity to RIG1 (as RIG1 is expressed in the human species only). Whether the mechanism of differentiation induced by mouse

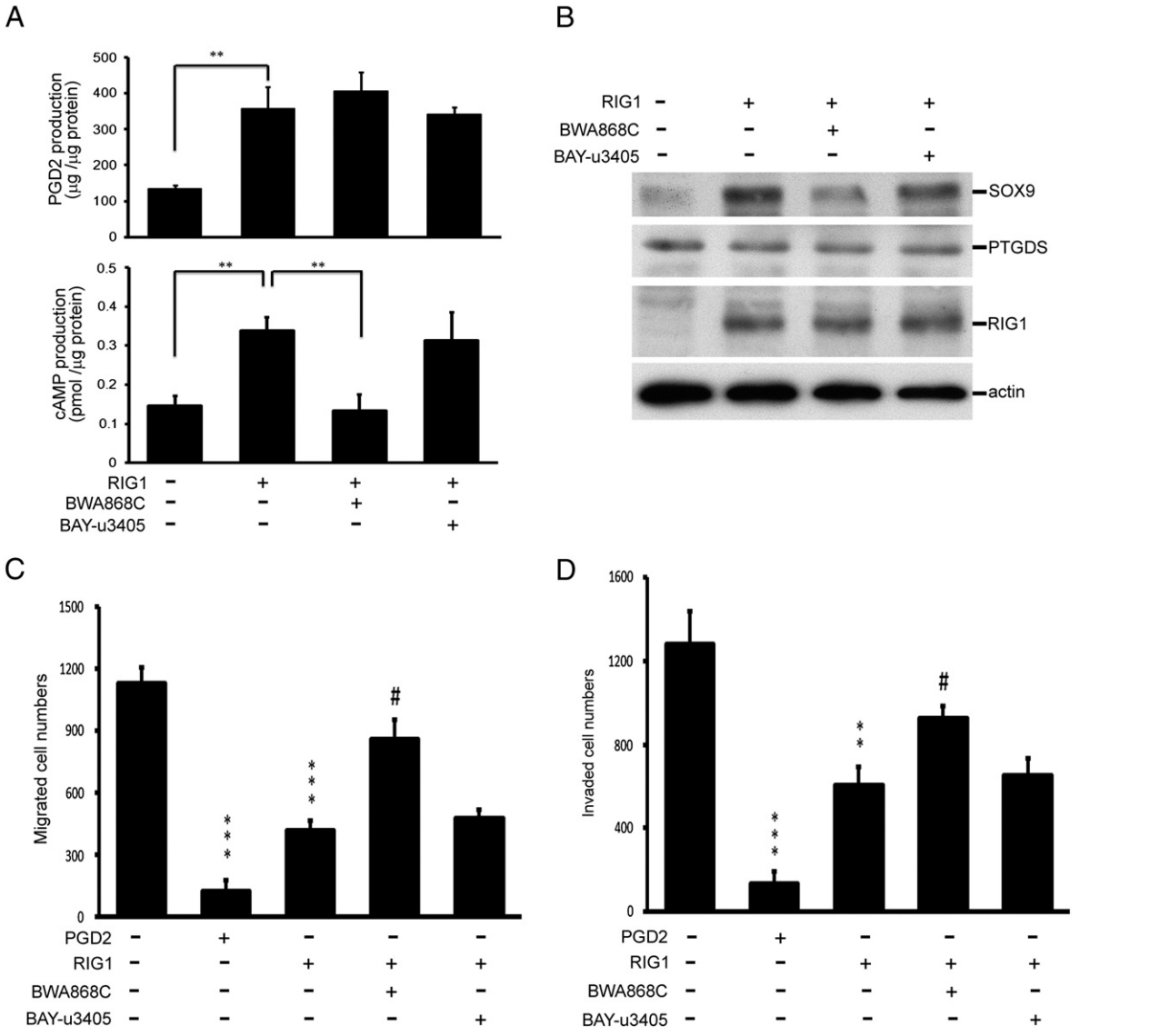

Fig. 6. PGD2 DP1 antagonist alleviates the RIG1-mediated suppression of migration and invasion. NT2/D1 cells were transfected with RIG1 and incubated with 10 μM BWA868C or BAY-u3405 for 24 h. Cell lysates were prepared, and the expression of PGD2, cAMP, or SOX9 was determined by enzyme immunoassay (A) and immunoblotting (B). NT2/D1 cell lysates were treated with 500 ng/mL PGD2 or transfected with RIG1 expression vector and incubated with 10 μM BWA868C or BAY-u3405 for 24 h. The cells were added in triplicate in upper polycarbonate membrane inserts in 24-well plates. Lower wells contained 700 μL of DMEM with 20% FBS, which was used as chemoattractant. Migratory cells were stained after 24 h of incubation (C). Invasiveness was measured with the Matrigel invasion assay after 72 h of incubation (D). BWA868C or BAY-u3405 was present during migration and invasion. Representative results of three independent experiments are shown. Student's t-test: **, $P<0.01$; ***, $P<0.001$.

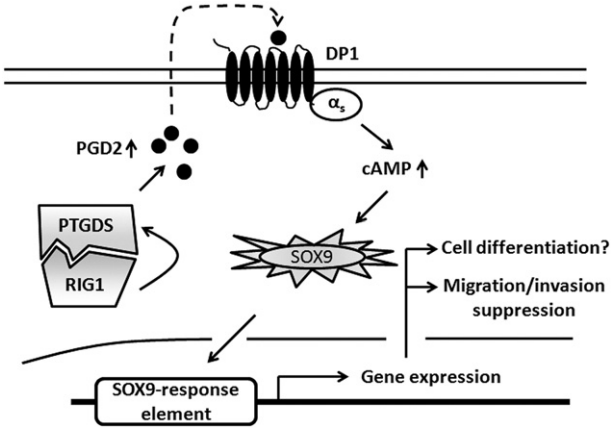

Fig. 7. Proposed model of the RIG1/PTGDS pathway. This schematic representation depicts that PTGDS is enhanced by RIG1 to increase PGD2, triggers the PGD2 DP1/cAMP/SOX9 signaling pathways, and then suppresses cell migration and invasion or induces cell differentiation.

H-rev107 is similar to that of PGD2, which is mediated through the regulation of SOX9 gene expression, as proposed by Malki et al. [25], needs further investigation.

Aside from RAS suppression, previous studies seem to indicate that RIG1-mediated cell differentiation and cancer suppression result in a modulate expression or activity such as HER2, PI3K/AKT, mTOR, or tissue transglutaminase I [12,13,43]. These observations suggest that RIG1 has multiple functions in various tissues and that the different signal pathways involved in RIG1-mediated cell differentiation/cellular apoptosis might be due to the difference in specific binding protein. Regardless of specific downstream signaling, most results from previous studies demonstrate that C-terminus is required for HREV107 protein family-mediated cell differentiation and apoptosis [10,13,26,27,44]. Truncation of RIG1 at the C-terminus (RIGΔC) results in complete loss of the activity that binds PTGDS and then activates the PGD2 signal pathway, although RIGΔC has the NC domain. In addition, different truncated RIG1 variants are distributed differently within a cell [26]. It

becomes difficult to perform domain mapping of the RIG1–PTGDS complex in vivo under these circumstances.

Our findings provide insights into the molecular mechanism by which RIG1 enhances PTGDS, thus regulating cancer invasion and metastasis. The finding that RIG1 forms a complex with PTGDS to mediate the PGD2 signaling pathway and suppress cancer cell invasion may offer new targets for treatments to prevent cancer metastasis.

Supplementary data to this article can be found online at http://dx.doi.org/10.1016/j.bbamcr.2012.08.013.

Acknowledgements

This work was supported by grants from the National Science Council (NSC 97-2311-B-303-001, NSC 100-2311-B-303-001) and the Buddhist Tzu Chi General Hospital, Taipei Branch (TCRD-TPE-101-23). The authors thank the Core Laboratory of the Buddhist Tzu Chi General Hospital Taipei Branch for facility support.

References

[1] S.L. Huang, R.Y. Shyu, M.Y. Yeh, S.Y. Jiang, Cloning and characterization of a novel retinoid-inducible gene 1(RIG1) deriving from human gastric cancer cells, Mol. Cell. Endocrinol. 159 (2000) 15–24.
[2] D. DiSepio, C. Ghosn, R.L. Eckert, A. Deucher, N. Robinson, M. Duvic, R.A. Chandraratna, S. Nagpal, Identification and characterization of a retinoid-induced class II tumor suppressor/growth regulatory gene, Proc. Natl. Acad. Sci. U. S. A. 95 (1998) 14811–14815.
[3] B. Casanova, M.T. de la Fuente, M. Garcia-Gila, L. Sanz, A. Silva, J.A. Garcia-Marco, A. Garcia-Pardo, The class II tumor-suppressor gene RARRES3 is expressed in B cell lymphocytic leukemias and down-regulated with disease progression, Leukemia 15 (2001) 1521–1526.
[4] V. Anantharaman, L. Aravind, Evolutionary history, structural features and biochemical diversity of the NlpC/P60 superfamily of enzymes, Genome Biol. 4 (2003) R11.
[5] P.J. Hughes, G. Stanway, The 2A proteins of three diverse picornaviruses are related to each other and to the H-rev107 family of proteins involved in the control of cell proliferation, J. Gen. Virol. 81 (2000) 201–207.
[6] A. Hajnal, R. Klemenz, R. Schafer, Subtraction cloning of H-rev107, a gene specifically expressed in H-ras resistant fibroblasts, Oncogene 9 (1994) 479–490.
[7] K. Husmann, C. Sers, E. Fietze, A. Mincheva, P. Lichter, R. Schafer, Transcriptional and translational downregulation of H-REV107, a class II tumour suppressor gene located on human chromosome 11q11-12, Oncogene 17 (1998) 1305–1312.
[8] H. Akiyama, Y. Hiraki, M. Noda, C. Shigeno, H. Ito, T. Nakamura, Molecular cloning and biological activity of a novel Ha-Ras suppressor gene predominantly expressed in skeletal muscle, heart, brain, and bone marrow by differential display using clonal mouse EC cells, ATDC5, J. Biol. Chem. 274 (1999) 32192–32197.
[9] H. Ito, H. Akiyama, C. Shigeno, T. Nakamura, Isolation, characterization, and chromosome mapping of a human A-C1 Ha-Ras suppressor gene (HRASLS), Cytogenet. Cell Genet. 93 (2001) 36–39.
[10] F.M. Tsai, R.Y. Shyu, S.Y. Jiang, RIG1 inhibits the Ras/mitogen-activated protein kinase pathway by suppressing the activation of Ras, Cell. Signal. 18 (2006) 349–358.
[11] F.M. Tsai, R.Y. Shyu, S.Y. Jiang, RIG1 suppresses Ras activation and induces cellular apoptosis at the Golgi apparatus, Cell. Signal. 19 (2007) 989–999.
[12] M.T. Sturniolo, R.A. Chandraratna, R.L. Eckert, A novel transglutaminase activator forms a complex with type 1 transglutaminase, Oncogene 24 (2005) 2963–2972.
[13] M.T. Sturniolo, S.R. Dashti, A. Deucher, E.A. Rorke, A.M. Broome, R.A. Chandraratna, T. Keepers, R.L. Eckert, A novel tumor suppressor protein promotes keratinocyte terminal differentiation via activation of type I transglutaminase, J. Biol. Chem. 278 (2003) 48066–48073.
[14] M. Duvic, B. Helekar, C. Schulz, M. Cho, D. DiSepio, C. Hager, D. DiMao, P. Hazarika, B. Jackson, J. Breuer-McHam, J. Young, G. Clayman, S.M. Lippman, R.A. Chandraratna, N.A. Robinson, A. Deucher, R.L. Eckert, S. Nagpal, Expression of a retinoid-inducible tumor suppressor, tazarotene-inducible gene-3, is decreased in psoriasis and skin cancer, Clin. Cancer Res. (2000) 3249–3259.
[15] S. Siegrist, C. Feral, M. Chami, B. Solhonne, M.G. Mattei, E. Rajpert-De Meyts, G. Guellaen, F. Bulle, hH-Rev107, a class II tumor suppressor gene, is expressed by post-meiotic testicular germ cells and CIS cells but not by human testicular germ cell tumors, Oncogene 20 (2001) 5155–5163.
[16] R.Y. Shyu, S.Y. Jiang, J.M. Chou, Y.L. Shih, M.S. Lee, J.C. Yu, P.C. Chao, Y.J. Hsu, S.W. Jao, RARRES3 expression positively correlated to tumour differentiation in tissues of colorectal adenocarcinoma, Br. J. Cancer 89 (2003) 146–151.
[17] K. Lotz, T. Kellner, M. Heitmann, I. Nazarenko, A. Noske, A. Malek, A. Gontarewicz, R. Schafer, C. Sers, Suppression of the TIG3 tumor suppressor gene in human ovarian carcinomas is mediated via mitogen-activated kinase-dependent and -independent mechanisms, Int. J. Cancer 116 (2005) 894–902.
[18] C. Sers, U. Emmenegger, K. Husmann, K. Bucher, A.C. Andres, R. Schafer, Growth-inhibitory activity and downregulation of the class II tumor-suppressor gene H-rev107 in tumor cell lines and experimental tumors, J. Cell Biol. 136 (1997) 935–944.
[19] S.L. Huang, R.Y. Shyu, M.Y. Yeh, S.Y. Jiang, The retinoid-inducible gene I: effect on apoptosis and mitogen-activated kinase signal pathways, Anticancer Res. 22 (2002) 799–804.
[20] R.E. Duncan, E. Sarkadi-Nagy, K. Jaworski, M. Ahmadian, H.S. Sul, Identification and functional characterization of adipose-specific phospholipase A2 (AdPLA), J. Biol. Chem. 283 (2008) 25428–25436.
[21] T. Uyama, X.H. Jin, K. Tsuboi, T. Tonai, N. Ueda, Characterization of the human tumor suppressors TIG3 and HRASLS2 as phospholipid-metabolizing enzymes, Biochim. Biophys. Acta 1791 (2009) 1114–1124.
[22] W.L. Smith, D.L. DeWitt, R.M. Garavito, Cyclooxygenases: structural, cellular, and molecular biology, Annu. Rev. Biochem. 69 (2000) 145–182.
[23] S. Narumiya, Y. Sugimoto, F. Ushikubi, Prostanoid receptors: structures, properties, and functions, Physiol. Rev. 79 (1999) 1193–1226.
[24] I.R. Adams, A. McLaren, Sexually dimorphic development of mouse primordial germ cells: switching from oogenesis to spermatogenesis, Development 129 (2002) 1155–1164.
[25] S. Malki, S. Nef, C. Notarnicola, L. Thevenet, S. Gasca, C. Mejean, P. Berta, F. Poulat, B. Boizet-Bonhoure, Prostaglandin D2 induces nuclear import of the sex-determining factor SOX9 via its cAMP-PKA phosphorylation, EMBO J. 24 (2005) 1798–1809.
[26] F.M. Tsai, R.Y. Shyu, S.C. Lin, C.C. Wu, S.Y. Jiang, Induction of apoptosis by the retinoid inducible growth regulator RIG1 depends on the NC motif in HtTA cervical cancer cells, BMC Cell Biol. 10 (2009) 15.
[27] R.Y. Shyu, Y.C. Hsieh, F.M. Tsai, C.C. Wu, S.Y. Jiang, Cloning and functional characterization of the HRASLS2 gene, Amino Acids 35 (2008) 129–137.
[28] S.T. Reddy, M.V. Winstead, J.A. Tischfield, H.R. Herschman, Analysis of the secretory phospholipase A2 that mediates prostaglandin production in mast cells, J. Biol. Chem. 272 (1997) 13591–13596.
[29] H. Fujishima, R.O. Sanchez Mejia, C.O. Bingham III, B.K. Lam, A. Sapirstein, J.V. Bonventre, K.F. Austen, J.P. Arm, Cytosolic phospholipase A2 is essential for both the immediate and the delayed phases of eicosanoid generation in mouse bone marrow-derived mast cells, Proc. Natl. Acad. Sci. U. S. A. 96 (1999) 4803–4807.
[30] B. Moniot, F. Declosmenil, F. Barrionuevo, G. Scherer, K. Aritake, S. Malki, L. Marzi, A. Cohen-Solal, I. Georg, J. Klattig, C. Englert, Y. Kim, B. Capel, N. Eguchi, Y. Urade, B. Boizet-Bonhoure, F. Poulat, The PGD2 pathway, independently of FGF9, amplifies SOX9 activity in Sertoli cells during male sexual differentiation, Development 136 (2009) 1813–1821.
[31] P.J. Baker, P.J. O'Shaughnessy, Expression of prostaglandin D synthetase during development in the mouse testis, Reproduction 122 (2001) 553–559.
[32] A. Zhang, Z. Dong, T. Yang, Prostaglandin D2 inhibits TGF-beta1-induced epithelial-to-mesenchymal transition in MDCK cells, Am. J. Physiol. Renal Physiol. 291 (2006) F1332–F1342.
[33] T. Yoshida, S. Ohki, M. Kanazawa, H. Mizunuma, Y. Kikuchi, H. Satoh, Y. Andoh, A. Tsuchiya, R. Abe, Inhibitory effects of prostaglandin D2 against the proliferation of human colon cancer cell lines and hepatic metastasis from colorectal cancer, Surg. Today 28 (1998) 740–745.
[34] D. Wang, R.N. Dubois, Eicosanoids and cancer, Nat. Rev. Cancer 10 (2010) 181–193.
[35] T. Passeron, J.C. Valencia, T. Namiki, W.D. Vieira, H. Passeron, Y. Miyamura, V.J. Hearing, Upregulation of SOX9 inhibits the growth of human and mouse melanomas and restores their sensitivity to retinoic acid, J. Clin. Invest. 119 (2009) 954–963.
[36] M. Ueno, J. Nakashima, T. Nakanoma, T. Ohigashi, R. Hirata, M. Iida, M. Suzuki, M. Sano, Y. Yamada, N. Deguchi, Retinoic acid-induced cell growth inhibition and differentiation in testicular carcinoma cells in culture, Hum. Cell 10 (1997) 151–158.
[37] W.H. Miller Jr., D. Moy, A. Li, J.F. Grippo, E. Dmitrovsky, Retinoic acid induces down-regulation of several growth factors and proto-oncogenes in a human embryonal cancer cell line, Oncogene 5 (1990) 511–517.
[38] S. Ling, X. Chang, L. Schultz, T.K. Lee, A. Chaux, L. Marchionni, G.J. Netto, D. Sidransky, D.M. Berman, An EGFR-ERK-SOX9 signaling cascade links urothelial development and regeneration to cancer, Cancer Res. 71 (2011) 3812–3821.
[39] L. Zhao, G. Li, G.Q. Zhou, SOX9 directly binds CREB as a novel synergism with the PKA pathway in BMP-2-induced osteochondrogenic differentiation, J. Bone Miner. Res. 24 (2009) 826–836.
[40] A. Kobayashi, H. Chang, M.C. Chaboissier, A. Schedl, R.R. Behringer, Sox9 in testis determination, Ann. N. Y. Acad. Sci. 1061 (2005) 9–17.
[41] D. Wilhelm, R. Hiramatsu, H. Mizusaki, L. Widjaja, A.N. Combes, Y. Kanai, P. Koopman, SOX9 regulates prostaglandin D synthase gene transcription in vivo to ensure testis development, J. Biol. Chem. 282 (2007) 10553–10560.
[42] R.L. Gerena, N. Eguchi, Y. Urade, G.J. Killian, Stage and region-specific localization of lipocalin-type prostaglandin D synthase in the adult murine testis and epididymis, J. Androl. 21 (2000) 848–854.
[43] C.C. Ou, S.C. Hsu, Y.H. Hsieh, W.L. Tsou, T.C. Chuang, J.Y. Liu, M.C. Kao, Downregulation of HER2 by RIG1 involves the PI3K/Akt pathway in ovarian cancer cells, Carcinogenesis 29 (2008) 299–306.
[44] A. Deucher, S. Nagpal, R.A. Chandraratna, D. Di Sepio, N.A. Robinson, S.R. Dashti, R.L. Eckert, The carboxy-terminal hydrophobic domain of TIG3, a class II tumor suppressor protein, is required for appropriate cellular localization and optimal biological activity, Int. J. Oncol. 17 (2000) 1195–1203.